Article:
Archer, R.A., Howse, J.R., Fujii, S. et al. (2020) pH-responsive catalytic janus motors with autonomous navigation and cargo-release functions. Advanced Functional Materials, 30 (19). 2000324. ISSN: 1616-301X

https://doi.org/10.1002/adfm.202000324

pH Responsive Catalytic Janus Motors with Autonomous Navigation and Cargo Release Functions

R. A. Archer,[a] J. R. Howse,[a] S. Fujii,[b,c] H. Kawashima,[d] G. A. Buxton,[e] S. J. Ebbens[a]*

[a]Department of Chemical and Biological Engineering, University of Sheffield - Sheffield, S1 3JD, United Kingdom

[b]Department of Applied Chemistry, Faculty of Engineering, Osaka Institute of Technology, 5-16-1 Omiya, Asahi-ku, Osaka 535-8585, Japan

[c]Nanomaterials Microdevices Research Center, Osaka Institute of Technology, 5-16-1 Omiya, Asahi-ku, Osaka 535-8585, Japan

[d]Division of Applied Chemistry, Graduate School of Engineering, Osaka Institute of Technology, 5-16-1 Omiya, Asahi-ku, Osaka 535-8585, Japan

[e]Department of Science, Robert Morris University, Moon Township, PA 15108, USA

Abstract

This paper demonstrates the ability to make multi-functional polymeric Janus colloids that display catalytically driven propulsion, change their size in response to local variations in pH and vary cargo release rate. Systematic investigation of the colloidal trajectories reveals that in acidic environments the propulsion velocity reduces dramatically due to the colloid swelling. This leads to a chemotaxis like accumulation for ensembles of these responsive particles in low pH regions. In synergy with this chemically defined accumulation, the colloids also show an enhancement in the release rate of an encapsulated cargo molecule. Together, these effects result in a strategy to harness catalytic propulsion for combined autonomous transport and cargo release directed by a chemical stimulus, displaying a greater than 30 times local cargo accumulation enhancement. Lactic acid can be used as the stimulus for this behaviour, an acid produced by some tumours', suggesting possible eventual utility as a drug delivery method. Applications for microfluidic transport are also discussed.

Keywords

Colloids, Stimuli-Responsive Materials, Microfluidics, Drug Delivery

Introduction

Catalytic Janus colloids are well known for their ability to produce rapid enhanced self-propulsive motion in solutions by decomposing surrounding dissolved fuel molecules.[1] Much attention has been devoted to harnessing this catalytic motion to enable new approaches to microfluidic transport.[2–5] One particularly exciting idea is to develop Janus colloids that can autonomously navigate to a specific target and release an encapsulated cargo. This capacity could be used for transport within microfluidic devices, or to deliver drugs to therapeutic targets in the body. Based on this overall goal, methods have been developed that can direct and control the motion of catalytic Janus colloids,[6] and equip them with cargo carrying and releasing capacities.[7] Directing motion requires overcoming the intrinsically diffusive nature of unconstrained colloids. Various approaches have been investigated to achieve this including alignment using external[7] or naturally occurring fields[8] and steering by topographical features.[9,10] However in order to enable navigation to a specific target, mimicking the chemotaxis phenomena displayed by micro-organisms appears particularly promising. Chemotaxis is possible because micro-organisms can alter their motion based on their ability to sense chemical gradients, resulting in collective accumulations around locally high or low concentrations of a particular stimulus, such as a nutrient.[11] This approach is attractive to emulate, as establishing a

synthetic analogue would allow cargo carrying colloids to concentrate in a certain location without recourse to external monitoring and guidance. A chemotaxis analogue would also allow the colloids to respond dynamically to changes in the position and distribution of the chemical stimuli. To give one potential context for the utility of this strategy, many therapeutic targets produce local chemical gradients[12] which could be used to guide a suitable drug delivery system.

To date, motivated by this goal, experimental reports for chemotaxis like behaviour in synthetic motile catalytic colloidal systems have demonstrated statistical accumulations of colloids relative to chemical gradients.[13] The way in which gradients modify individual colloid trajectories to produce this effect has also been investigated.[14] However, in these examples, navigation requires the chemical "bread-crumb" trail to be provided by fuel concentration variations, i.e. the reagent being decomposed to producing the catalytic motion. This is a significant restriction, and limits the scenarios in which this phenomena could be used. Addressing this limitation, we previously demonstrated (*in-silico*) the potential, to also produce a chemotaxis like behaviour in response to pH gradients within a constant fuel concentration environment by exploiting motile size changing hydrogel Janus colloids.[15] This approach has direct relevance to medicine, as tumour cells produce pH gradients in their surroundings.[12]

The second challenge is to incorporate and release cargo from motile catalytic colloids. This has also been demonstrated in a number of experimental systems. For example, magnetic colloidal cargo has been attached and released from the surface of bi-metallic nanorods,[16] while various other tethering strategies for cargo attachment,[3] including those that selectively bind specific cargo have been reported.[17] Another strategy is to store cargo within the motile colloids. Recently, using this approach it was shown that motile colloids made from mesoporous silica can be loaded with small molecules,[18] and that these colloids will self-concentrate within one compartment of a specifically designed heart shaped cell. A follow up study separately reported enhanced release of the absorbed cargo molecules in the presence of the motion producing fuel.[19] These demonstrations represent important steps towards the goal of achieving autonomous cargo release in response to a chemical stimulus. However, the increase in release rate relied on changes in fuel concentration, and navigation was achieved using topographical rather than chemical guidance.

Expanding on this progress, the work presented here aims to investigate the potential to combine the previously proposed pH responsive Janus colloids navigation strategy with an accompanying pH triggered release of molecular cargo trapped within the colloids body. If successful, this could allow cargo carrying colloids to both autonomously accumulate and display enhanced cargo release rate at a chemically defined location. Our previous simulation demonstrating pH gradient navigation was based on polymethacrylic acid (PMAA), a material that swells at higher pH's. Simulations showed that catalytically motile PMAA Janus colloids accumulate in high pH regions, mainly due to a reduction in translational velocity when swollen.[15] This finding is promising for targeted cargo release, as the associated porosity increase in the swollen state may also enhance the release rate of any absorbed molecules.

Due to a particular eventual application area for these transporters being drug delivery to a tumour, which is known to have an acidic micro-environment, here we investigated the behaviour of poly(2-vinyl pyridine) (PVP) colloids, which shows the inverse behaviour to PMAA: swelling at low, acidic pH's, Figure 1b. Based on our previous simulations, and the expected controlled release behaviour, this material could both accumulate and show enhanced release in low pH regions, Figure 1a. However, the previous simulations relied on theoretical predictions for the effect of changing colloidal size on propulsion without any direct experimental measurements from pH responsive motile colloids. Importantly, these predictions did not assess changes in surface mobility parameters that occur during

swelling,[20] which could also influence the catalytic propulsion mechanism. Consequently, it remains desirable to develop an experimentally accessible size changing motile system where the effect of pH on motion can be directly observed.

In this context, to strengthen the case for pH responsive active transport and release, this study investigates PVP colloids, appropriately functionalised on one side with platinum catalyst, that experimentally demonstrate catalytic motility powered by the decomposition of hydrogen peroxide. This system allows us to systematically investigate and interpret the effect of pH changes on colloid translational and rotational propulsion. In the experiments, pH is varied using both nitric and lactic acid. Lactic acid is produced by tumour cells,[21] representing a biologically important signalling chemical. In addition, the pH dependant release rate of a model encapsulated dye molecule (Rhodamine) contained within the PVP colloids is determined. Based on this experimental data, we construct new simulations to investigate the statistical accumulation of these responsive cargo carrying colloids in response to pH gradients. These simulations reveal the exciting potential to experimentally access combined navigation and targeted release functions.

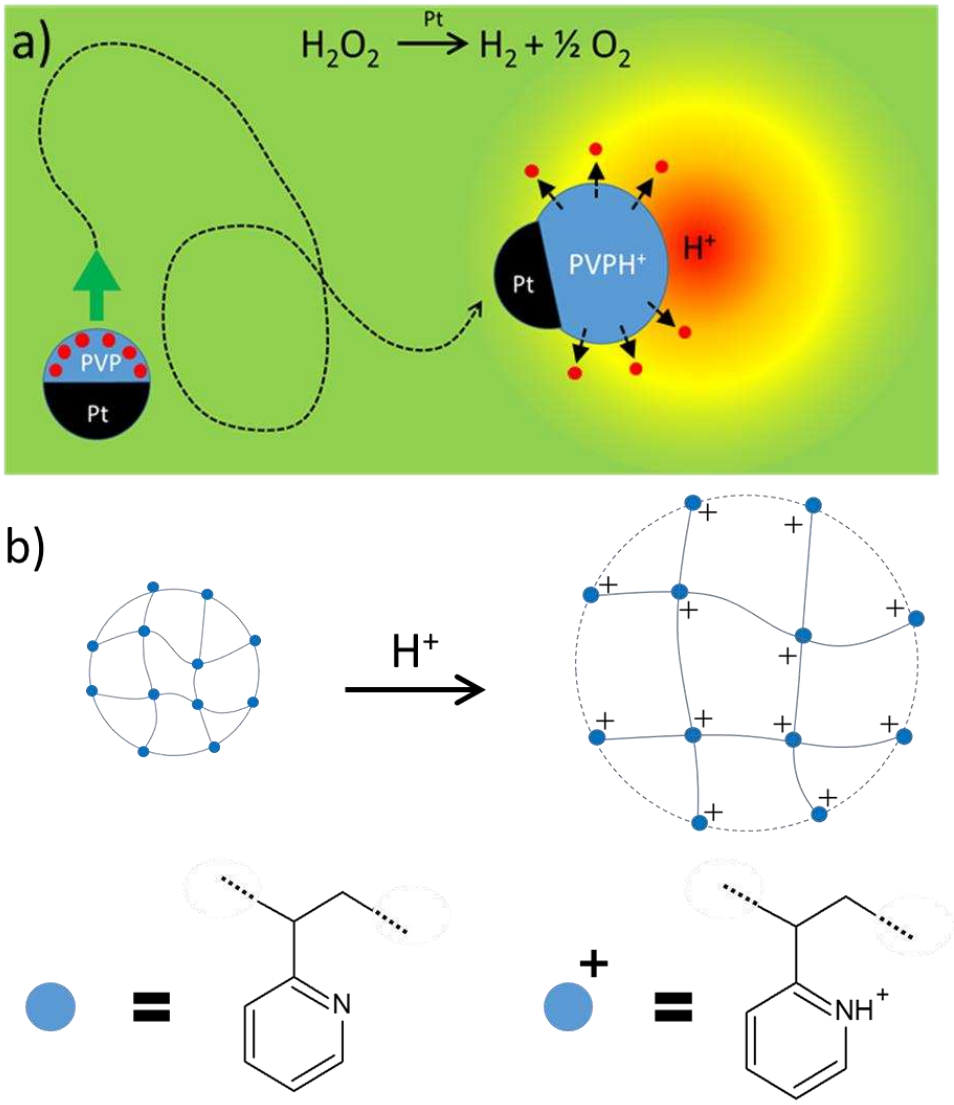

Figure 1. (a) Schematic of the proposed size changing transport mechanism. PVP colloids are coated with platinum on one hemisphere, generating motion by catalytically decomposing hydrogen peroxide. As pH decreases, PVP colloids swell (See Figure 1b), modulating their trajectories to result in a

statistical accumulation relative to a pH gradient. Simultaneously, the swelling increases the release rate of encapsulated cargo molecules (shown by red dots) (b) Schematic of the structural origin of PVP colloids size changes. At low pH the Nitrogen in the pyridine ring becomes protonated, and the resulting electrostatic repulsion causes the polymeric network to swell.

Method

Materials

2-Vinylpyridine (2-VP), divinylbenzene (DVB), Aliquat 336, 2,2'-Azobis(2-methylpropionamidine)dihydrochloride. Monomethoxy-capped poly(ethylene glycol) methacrylate (PEGMA) and polystyrene Fluoromax colloids (1 µm diameter) were supplied by Thermo Fisher scientific and used as received. Lactic acid, Nitric acid, Hydrogen Peroxide and Rhodamine B were supplied by Sigma Aldrich and used as supplied. Deionised water was obtained from a Elga Pureflex 3 system (>18.2 MΩ resistivity). The platinum target for sputter coating was supplied by Agar Scientific.

pH responsive colloid synthesis.

PVP colloids were prepared as previously described by Dupin et al.[22] Briefly: 2-VP, DVB, Aliquat 336 and PEGMA were dissolved in deionised water under an inert nitrogen atmosphere. The solution was stirred magnetically at 60 ^{o}C for 24 hrs after the initiator 2,2'-Azobis(2-methylpropionamidine) dihydrochloride (dissolved in deionised water) was added.

The formed colloids were collected and washed by repeated centrifugation cycles, removing the supernatant and re-dispersing into fresh deionised water to remove unreacted reagent and the initiator.

Active colloid synthesis

PVP and PS colloids were diluted to a low concentration suspension in ethanol. The dilute suspension was then spun coat (Laurell Technologies spin coater) onto clean glass microscope slides at 2000 rpm. Colloids dispersed on the glass slide were sputter coated (Agar Scientific Manual Sputter Coater) with 40 mA current under 40 mbar of argon for 12 seconds at a distance of 15 mm from a platinum target.

pH calibration

pH calibration curves were prepared using a Mettler Toledo FiveEasy benchtop pH meter to measure the pH of a series of known concentrations of lactic and nitric acid in deionised water and hydrogen peroxide (10% wt/v). OriginPro was used to apply a curve fit to the measured data and this expression was used to determine the solution composition required to result in the desired pH for each experiment.

Colloid Sizing and Tracking

Colloids were transferred to solution by rubbing wetted lens tissue onto the colloid deposited glass slides. The lens tissue was shaken in a small volume of deionised water, which is then separated from the tissue resulting in a low concentration of the desired colloids suspended in deionised water.

For the initial analysis of pH induced size changes, the suspension of colloids in deionised water was acidified to the desired pH by addition of lactic acid. For analysis of catalytically induced motion, hydrogen peroxide (30% wt/v) was also added in a 1:1 ratio to make a 15% H_2O_2 solution. After 20 minutes the hydrogen peroxide solution was further diluted to 10% H_2O_2. Solutions were acidified to the appropriate pH by appropriate additions of lactic or Nitric acid.

Motion analysis of the colloids was performed using a Nikon eclipse T-100 microscope equipped with a Pixelink PL-B742F camera. Videos of 1000 frames recorded at 33 fps at a resolution of 800x600 (0.33 pixels per micron) were taken of the colloids suspended in solutions. The videos were analysed using custom built software based on LabVIEW vision assistant which gives frame by frame *x*, *y* coordinates of the colloids. Mean square displacements (MSD) as a function of time step, *t* were calculated from these coordinates. The MSD versus time data was used to find the effect of pH change on the radius of colloids in the absence of fuel under the assumption that they were undergoing Brownian motion. This entailed determining the gradient of the MSD v time plot, to determine the Brownian translational diffusion coefficient, D and then using the Stoke-Einstein equation with appropriate fluid viscosity. The MSD versus time data for the fuelled catalytically active colloids was analysed as previously described to allow measures of translational velocity, angular velocity, *D* and the Brownian rotation coefficient to be extracted.[23] An in depth description of analysing MSD data for catalytic Janus colloid motion is found in Dunderdale et al.[24] A minimum of 36 separately observed trajectories were analysed in this manner for each condition investigated in order to arrive at the mean values for the four motion parameters reported in the results section.

Drug release profile

Suspensions of PVP colloids (200 mg) prepared as described above were incubated for 24 hours in a Rhodamine B solution (0.1 mM). The Rhodamine B incubated colloids were filtered by a milipore-filter set and washed with deionised water until the washings became clear. The washed PVP colloids that had been incubated with rhodamine-B were re-dispersed in deionised water to a total of 5ml volume by ultra-sonication to ensure complete re-dispersion. The 5ml volume was split into 5 equal 1 ml portions and the pH adjusted by lactic acid between pH 7.0 and pH 3.0. Periodically over 2 hours, the pH adjusted suspensions were centrifuged and the supernatant collected. The supernatant was then analysed by Ocean-optics USB2000 spectrometer with DT-mini-2-GS light source to determine the concentration of any released Rhodamine dye.

Simulations

We capture the random motion of the Janus colloids, and account for the diffusion and propulsion of these catalyst coated particles. Stokes dynamics dictate the evolution of the particle position and orientation, with the position, r, of a particle being updated using equation 1.

Equation 1: $$\epsilon_t \frac{\partial \vec{r}}{\partial t} = \vec{F} + \eta_t \vec{G}$$

Where $\epsilon_t = 6\,\pi\mu R$ is the friction coefficient, t is time, $\vec{F}$ is the propulsive force, $\eta_t = \sqrt{2\,\epsilon_t k_b T/\,\Delta t}$,($\Delta\ t$ is time step in simulation) and $\vec{G}$ is Gaussian noise with zero mean and unit variance. R is the radius of the particle, and T is temperature. Similarly, the orientation of the particle can also be updated using equation 2.

Equation 2: $$\epsilon_r \vec{\Omega} = \vec{T} + \eta_r \vec{G}$$

Where $\vec{\Omega}$ is the angular velocity and, $\vec{T}$, is the torque. The rotational frictional coefficient, $\epsilon_r = 8\pi\mu R^3$ and $\eta_r = \sqrt{2\,\epsilon_r k_b T/\Delta t)}$. The direction of the propulsive force and the direction of the torque are fixed relative to the particles rotation, and the particles rotation is described using quaternions (which involve four rotational angles, or quaternions, rather than three to avoid the singularities that can occur in Eulerian rotations). Therefore, the orientation of the particles are critical for determining the direction of their propulsion, and the timescales over which the particles rotate, and how far the particles travel in this time frame, are crucial to their accumulation in areas of low pH. The particle density is 1.56 x 10^{16} particles/m^3.

Results and Discussion

Initial experiments were performed to determine the magnitude of the pH responsive size changes for the as synthesised PVP colloids. As detailed in the methods section, this involved recording reference fuel free Brownian motion trajectories at different pH conditions, linear fitting of the mean-square displacements versus time data to arrive at a translational diffusion coefficient, and calculation of radius via the Stoke-Einstein equation. The radius calculations assumed spherical geometry: for Janus colloids this may not be the case, as is discussed in more detail below. Note that it is not possible to extract Brownian rotational rates from these non-propulsive reference trajectories. Figure 2 (red line) shows the change in colloid radius with change in pH. The PVP colloid starts to swell as the pH is reduced below 3.70. The mean PVP radius effectively doubles from pH 3.70 to 3.00, with the most significant size change occurring between pH 3.35 and pH 3.20. This is consistent with the previously documented behaviour of similarly synthesised colloids.[22] We note that swelling for similar PVP colloids has previously been reported to be reversible: swelling was found to be very rapid (5 ms) with de-swelling completing within 30 s.[25] After verifying that the PVP colloids were responsive to pH changes, attempts were made to make propulsive Janus colloids via asymmetrical metallisation with platinum on one face, using a variety of previously established methods. When metallisation was performed using electron beam induced thermal evaporation, although colloids did exhibit enhanced motion when placed in peroxide fuel, no size change as a function of pH was detected. This could indicate inadvertent cross-linking of the PVP had occurred during the metallisation process. In addition, a modification of our previously reported method to produce motile Janus colloids via platinum salt reduction[26] failed to result in detectable motion. In fact, only one approach, the use of low-pressure sputter coating, successfully produced PVP colloids that exhibited both enhanced motion in hydrogen peroxide, and pH responsive size changes. Figure 2 (blue line) shows the size response to pH changes for the sputter coated Janus PVP colloids that also show catalytic motility. These Pt coated PVP colloids show a dramatically reduced pH induced swelling response compared to the original PVP colloids, with a radius increase of only approximately 20 % from pH 3.70 to 3.00. This is a 10 fold reduction in swelling compared to the uncoated raw PVP colloids, and a distinct step-change in size is no longer seen. The reduction in swelling and change in profile is not surprising, due to the mechanical constraints imposed by the metal coating. However, due to the expected high sensitivity of catalytic Janus colloid translational velocity and Brownian rotational rate to changes in radius ($1/r$ and $1/r^3$ respectively),[27] even these reduced magnitude size changes are expected to be sufficient to both significantly modify propulsive trajectories, and also modify release rate of any absorbed cargo.

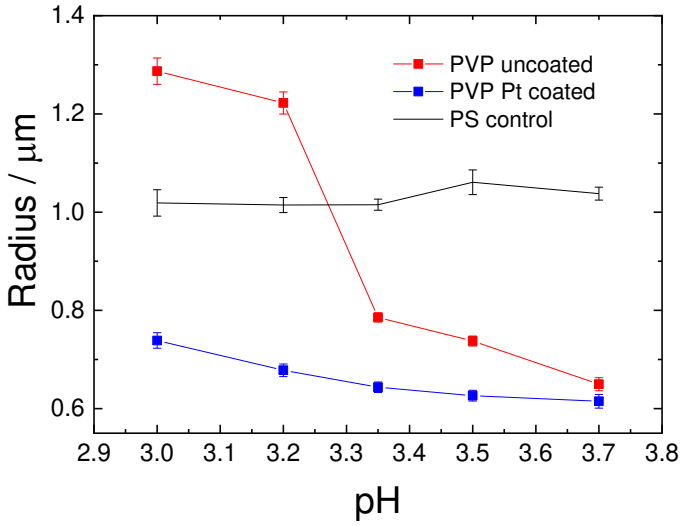

Figure 2: PVP radius as a function of pH for colloids before and after functionalisation with Pt. PS colloid radius as a function of pH is also shown. pH was controlled by the addition of lactic acid.

Having identified a successful manufacturing method for metallised Janus size changing colloids, a systematic statistical analysis of the effect of varying pH on the Pt coated PVP colloids' propulsive trajectories was performed. For comparison, similar analysis was also carried out for motile platinum coated Janus Polystyrene (PS) colloids, that did not exhibit any pH induced size changes (Figure 2, black line, nominal PS diameter as supplied is 1 µm). Figure 3 shows typical trajectories for Pt coated PS and Pt coated PVP colloids over 30 second periods in 10% H_2O_2 solutions with pH adjusted by the addition of lactic acid. The average displacement for Pt coated PS colloids from the origin over 30 seconds does not obviously decrease from pH 3.70 to 3.00. However, for Pt coated PVP, the trajectories are significantly altered by the change in pH, suggesting the pH responsive PVP is modulating the active colloids motility. The most apparent features are the decrease in overall average displacement from pH 3.70 to 3.35, and dramatic decrease in displacements from pH 3.35 to 3.00. As discussed in detail elsewhere, the trajectory of propulsive Janus colloids' is known to be determined by the magnitude of translational and rotational propulsion induced by the catalytic decomposition reaction, together with the rate of Brownian translational diffusion and rotation rate.[23] Based on this understanding, it is possible to use quantitative analysis of Mean-Square-Displacement (MSD) versus displacement graphs obtained from many *xy* trajectories to determine the average translational velocity, v, angular velocity, ω and Brownian diffusion coefficients. The short time step MSD regions that are used to determine the translational velocity, together with fits are shown in the Supplementary Information.

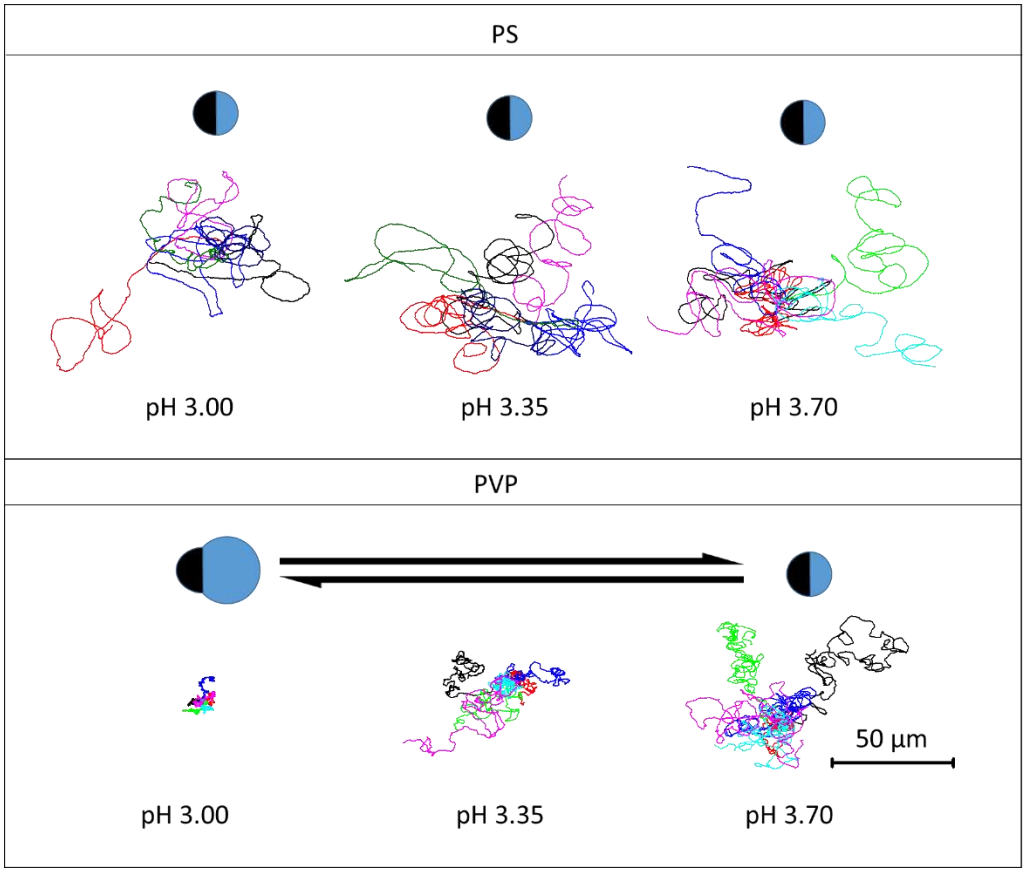

Figure 3. Representative trajectories (30 seconds) for polystyrene colloids (PS) and poly(2-vinyl pyridine) (PVP) colloids in 10% H_2O_2 with pH adjusted by addition of lactic acid to pH 3.70, pH 3.35 and pH 3.00.

In order to compare trends, the translational velocities were normalised against the translational velocity of a colloid in 10 % H_2O_2 with no addition of acid (pH 3.70). This allowed assessment of the comparative effect of the reduction of pH by the addition of either lactic or nitric acid to suspensions of platinum coated PS and PVP colloids. Considering these normalised translational velocities, it can be seen the PVP motile colloids' mean velocity is considerably more sensitive to decreasing pH than PS colloids, Figure 4a. PVP motile colloids show an approximate 40% reduction in translational velocity by pH 3.35, further continuing to a 70-80% reduction by pH 3.20 and finally, no translational propulsion is detected by pH 3.00 (i.e. the colloids become purely diffusive). PS based motile colloids show a gradual decrease in velocity between pH 3.70 and 3.00 for both lactic and nitric acid, losing approximately 40% of their initial velocity by pH 3.00. Interestingly there is no significant difference in the trend between the inorganic nitric acid and organic lactic acid despite the difference in molarity needed to reach a given pH value.

Previous mechanistic proposals suggest that the magnitude of propulsion for catalytic Janus colloids is influenced by the rate of fuel decomposition, and the surface mobility of both the active and catalytically inactive hemispheres of the colloid.[20] This later parameter, surface mobility, is currently poorly mapped to specific measurable surface parameters, but is understood to arise from a combination of surface properties including roughness, and surface chemistry. If these factors are held constant, propulsion velocity is also predicted to be modulated as the reciprocal of radius, a prediction that has been supported by experimental data.[27] For the PS based colloids, no size change is associated with changes in pH, Figure 2, and so the reduction in translational velocity can be

assigned solely to any changes in the decomposition rate of the peroxide fuel, and any surface mobility variations induced by the pH change. Considering surface mobility, in the absence of any strongly ionisable groups, dramatic changes in the surface chemistry of PS colloids are not expected over this pH range, and it is not likely that surface roughness changes appreciably, so a reaction rate change associated with the changing pH will be responsible for the reduced propulsion velocity.

The situation is considerably more complex for the PVP colloids. In addition to reaction rate changes, a size change is also occurring during acidification. To assess the correlation between the pH induced size change and observed trajectories, Figure 4b shows a comparative plot overlay of the pH induced radius and translational velocity changes for active PVP colloids in 10% H_2O_2. The reduction in the PVP motile colloids' translational velocity indeed appears to occur in tandem with the swelling. Based on the expected reciprocal relationship between radius and Janus colloids propulsion velocity, the radius change alone would only reduce the translational velocity by around 80 %. However, it is likely that surface mobility is also changing significantly: the swelling is symptomatic of a change in ionisation level within the PVP, and it is reasonable that surface roughness / porosity will also be modified by the size change. This combination of a change in surface charge and morphology are likely to alter the surface mobility for the exposed catalytically inactive PVP hemisphere of the colloid. One further possibility is that the Pt catalyst is also being effected by the expansion process, for example cracks may form if the mechanical integrity of the coating is lost during expansion. Direct observation of the coating during or after swelling has not been possible to investigate this factor. It is clear that together these factors result in a dramatic pH sensitive loss of propulsion velocity that is specifically associated with the pH response of PVP. However it is difficult to isolate the dominant contribution to the observed trajectory changes.

It was noted that the trajectories of the sputter coated motile colloids also showed additional driven rotations, indicating that the colloids were producing propulsive angular velocity. Figure 4c gives the values for the angular velocity, ω, as a function of pH, determined via MSD fitting. Note that angular velocity could not be determined at pH 3.00 for PVP based motile colloids as the MSD profiles were linear, indicating Brownian motion, which renders any driven rotations undetectable by trajectory analysis. It is clear that the angular velocity trends with pH are similar to those observed for translational velocity. Indeed, all the above arguments for the factors determining translational velocity apply to angular velocity. The origin of angular velocity in nominally symmetrical Janus colloids is thought to arise from small defects at the equatorial interface between catalyst and colloid that destroy this symmetry. The angular velocity observed here for sputter coated colloids is higher than that previously seen for Janus colloids prepared via thermal evaporation, suggesting less uniform coatings, likely due to the higher pressure associated with sputter coating resulting in shorter path lengths for the metal atoms, bluring the definition of the equator of the Janus colloid. In addition to these driven rotations, the Janus colloids also undergo stochastic Brownian rotations, which can be characterised by the Brownian rotation time, τ_R. Figure 4d displays the Brownian rotation time as determined by MSD fitting for the trajectories of motile PVP and PS catalytic colloids. The experimental values are compared with theoretical calculated values assuming spherical geometry, based on the radius values shown in Figure 2 (using $\tau_R = 8\pi\eta r^3/k_BT$, where η is viscosity, T temperature and k_B is Boltzmann's constant). The data shows a reasonable agreement with theory predictions, and in particular, an increase in τ_R associated with swelling is confirmed: the expanded particle are subject to slower Brownian rotation.[15] Again, τ_R cannot be determined for PVP catalytic colloids at pH 3.0 as they did not exhibit any translational propulsion. The ability to qualitatively discern the increase in persistence length that this leads to in the associated trajectories is hampered by the considerable driven angular rotations.

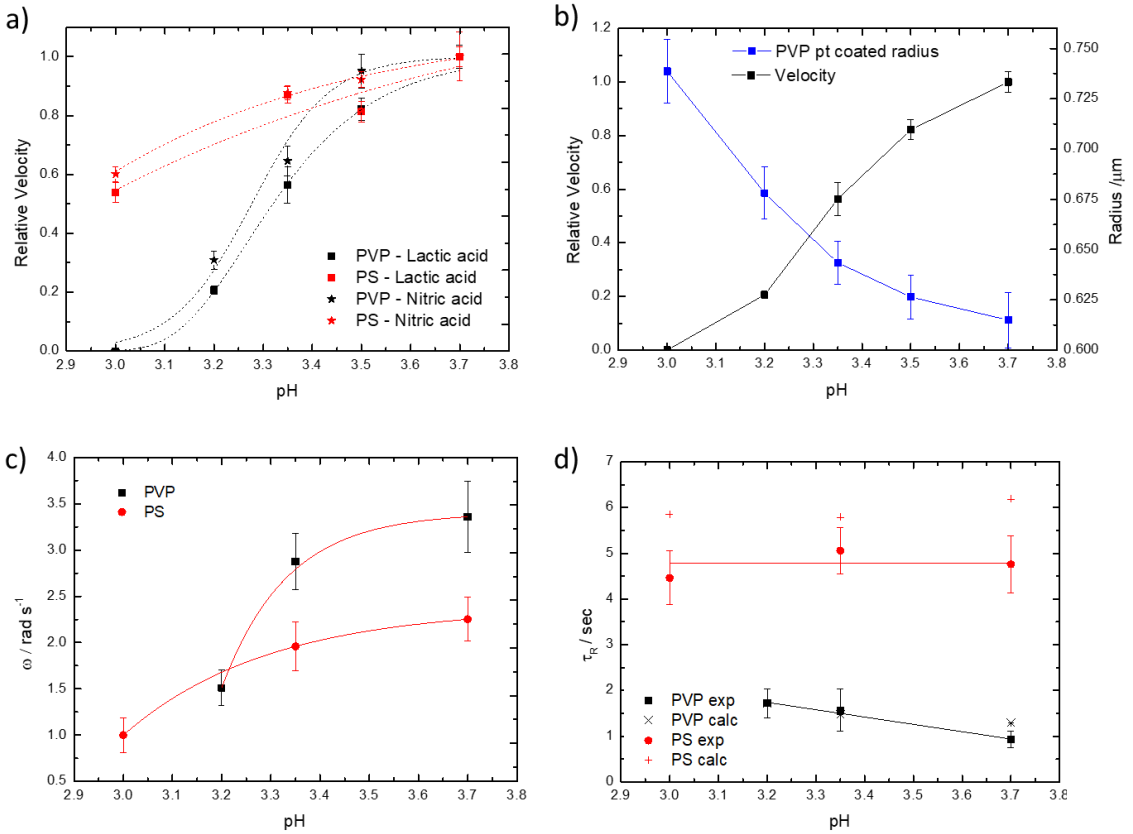

Figure 4 a) Average relative translational velocity for platinum coated PVP (black) and PS (Red) based motile colloids in 10% aqueous H_2O_2 with pH reduced by lactic acid (square) or nitric acid (star). Lines are the exponential fits used in the simulations. Note that the mean colloidal translation velocities at pH 3.7 were: PVP=11.4 μms^{-1} and PS=12.0 μms^{-1}. b) Combined plot of platinum coated PVP relative velocity (black) and radius against a common pH axis. c) adventitious angular velocity for PVP (black) and PS (red) as a function of pH in 10% H_2O_2 with pH controlled by lactic acid. Lines are exponential fits used in the simulations d) Brownian rotational constant for motile PVP and PS Janus colloids as a function of pH in 10% H_2O_2 with pH controlled by lactic acid. Calculated constants based on the colloidal size are also shown. Lines are linear best fits used in the simulations.

Having demonstrated an experimentally accessible motile size changing pH responsive colloidal system, the remainder of the paper explores the possibility to utilise this system to autonomously perform cargo delivery via both accumulating transporting colloids and modifying their cargo release rate in response to a pH gradient. Firstly, using simulations, an assessment of the response of many such colloids to a spherical pH gradient is made, to ascertain if the experimentally observed trajectory changes will lead to collective accumulations in low pH regions.

The spherical pH gradient region was chosen to have a radius of 50 μm and a pH of 3 inside the spherical region and 3.70 outside the spherical region. The gradual transition between the low and high pH volumes is described using a tanh function of the form:

$$pH = 3 + 0.35\left(1 + \tanh\left(\frac{(R - 50\ \mu m)}{10\ \mu m}\right)\right)$$

The effects of this pH variation on both PS and PVP colloids are depicted in Figure 5. Figure 5a shows the relative concentration (relative to the particles being randomly dispersed) of the PS particles as a function of the radial distance and time. For later times (after around 100 s) the particles can be seen

to accumulate in the spherical region (radial distance less than 50 µm). Concentrations of the PS particles are around twice that expected in systems where the particles are randomly distributed. The relative concentration of PVP particles are similarly shown in Figure 5b. In contrast to the system containing PS particles, the PVP particles accumulate over longer times but to much greater concentrations. It takes thousands of seconds for the particle concentrations to equilibrate and the concentration of particles in the spherical region reach values greater than twelve times what might be expected in systems where the particles are randomly distributed. In the earlier stages the responsive particles' accumulation is most pronounced in the region where the pH gradient is steepest.

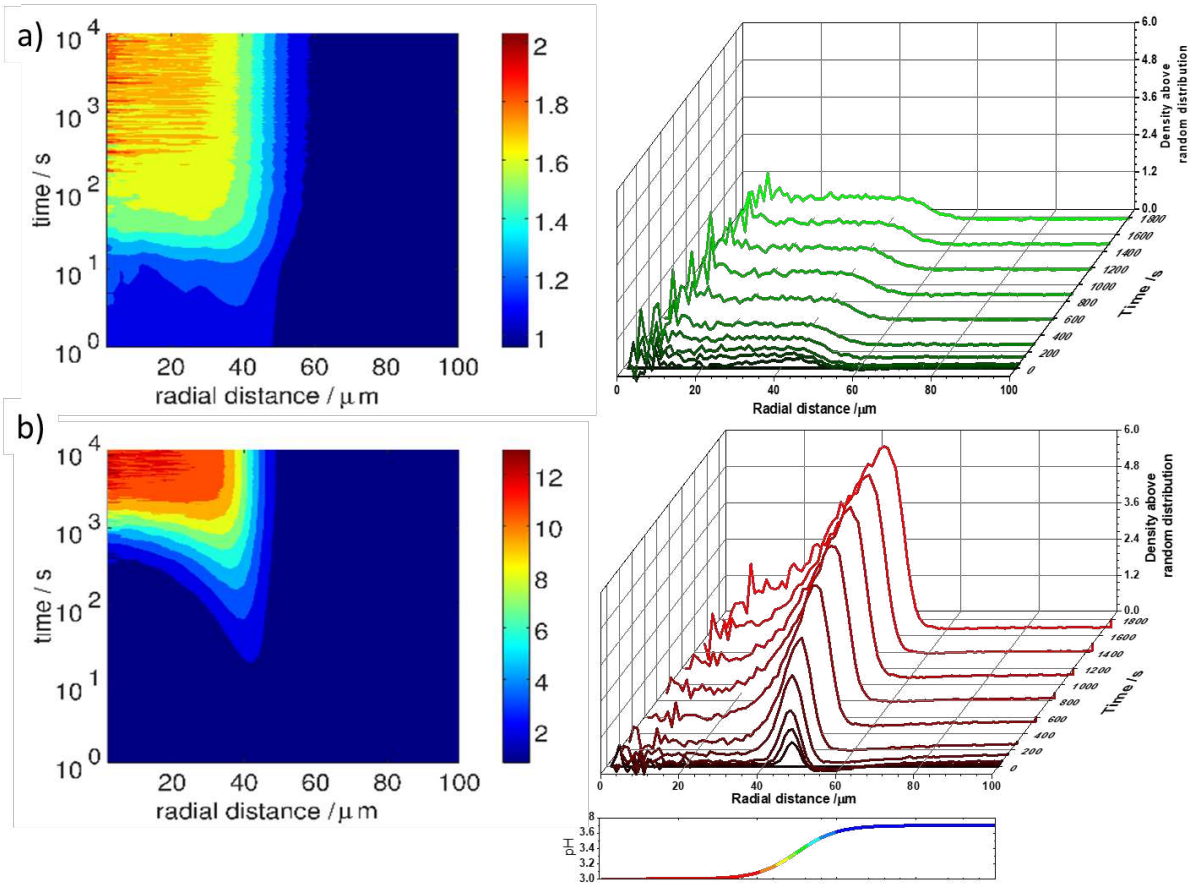

Figure 5: The relative density of a) PS and b) PVP particles as a function of radial distance and time. LHS, 2D colour maps on different z-scales. RHS, 3D plots of relative density on a common z-scale. The pH profile as a function of radial distance is also depicted below.

Finally, the effect of pH on the release rate of a model cargo molecule contained within the PVP colloids was experimentally determined, in order to ascertain if this accumulation behaviour would work in synergy with any triggered release displayed by the pH responsive material. The ability of PVP to show an environmentally triggered release of a loaded chemical was investigated by loading colloids with rhodamine B, chosen for its easily detectability with UV/Vis spectroscopy. Figure 6a shows the release profiles as a function of time for rhodamine B from PVP colloids in an aqueous solution with varying amounts of lactic acid added to adjust the pH. It is clear that larger amounts of dye have been released from the low pH, swollen PVP colloids at a given time, compared with the higher pH, un-swollen colloids. Figure 6b compares the rate of release of rhodamine B from the PVP colloids as a function of pH, after 30 minutes in suspension, showing that the release rate is clearly increased for the low pH swollen colloids. This data confirms the expected behaviour, that the more

porous swollen PVP state promotes faster cargo release. In particular, from, the pH of aqueous 10% H_2O_2 (pH 3.70) where the colloids show their highest propulsion velocity, to pH 3.0 where the PVP colloids have returned to Brownian diffusion, the rate of release of rhodamine B increases by more than a factor of two (from 0.06 nmol min^{-1} g^{-1} to 0.14 nmol min^{-1} g^{-1}).

A final simulation (Figure 6c) was performed to assess the combined effect of the pH gradient induced particle accumulation documented in Figure 5b, and the experimentally determined pH induced changes in dye release rate. To ensure the time-scales for both phenomena are realistically considered, the simulation commences with an even distribution of particles, displaying the initial experimental rhodamine B release rates (determined by differentiating Figure 6a and interpolating for pH). As the simulation proceeds, the rhodamine B release rates at a given pH evolve in time according to Figure 6a (again, by differentiation at the appropriate time point to determine rate, and interpolating for pH). The total accumulated amount of dye expected to have been released in a given position in the simulation at a given time is then calculated by multiplying the number of particles in that location by the current rate of release (the reported dye accumulation is normalised to the background accumulated dye concentration in a high pH background region of the simulation volume after 2 hours). Figure 6c clearly illustrates how the two enhancements to cargo delivery can work in tandem: a significant enhancement of PVP colloidal particle number density in the pH/lactic acid gradient region occurs due to size change induced modulation of colloidal motion (roughly 10 times the initial density after 2 hours), together with a further increase in the dye accumulation due to the faster release rate of the swollen PVP colloids. This analysis predicts that the synergy of these two effects will cause 30 times as much dye to accumulate in the spherical low pH region than outside this region over a 2 hour period.

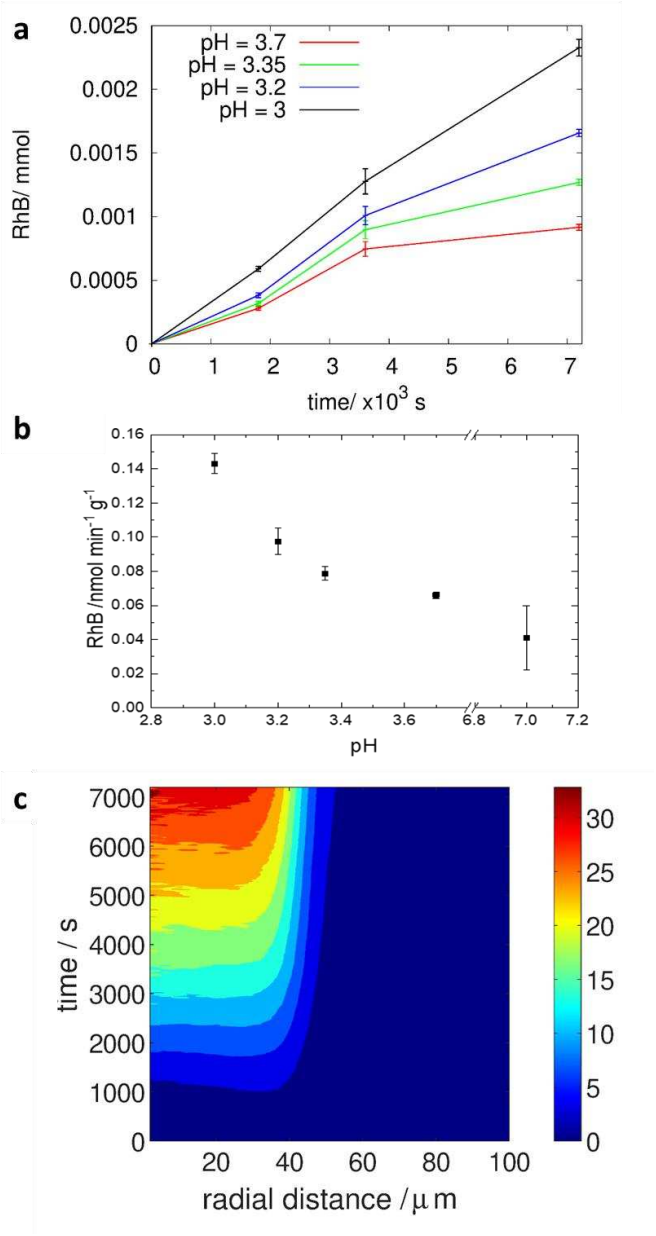

Figure 6. (a) Release profiles for rhodamine B (RhB) from RhB loaded PVP at different pH as a function of time (b) Release rate of rhodamine B (RhB) from RhB loaded PVP against pH of the solution after 30 minutes (c) The relative accumulation of rhodamine B as a function of radial distance (in the same pH gradient shown in Figure 5) due to the combined effect of colloidal accumulation and differential release rate (Figure 6a). Accumulation data was normalised against the background dye concentration at the end of the simulated time period.

Conclusions

We have developed catalytic Janus colloids based on Platinum functionalised PVP that display enhanced motility while undergoing pH induced size changes. To do so required careful optimisation of the metallisation procedure: employing low energy sputter coating was key to preserve the size changing response. Even with this optimisation, the degree of swelling observed for PVP colloids was considerably diminished after functionalisation with a hemi-spherical metal cap. This is likely due to mechanical constraint, combined with modifications of the PVP associated with the coating. Detailed investigation of the Pt-PVP colloids trajectories and motion parameters as a function of pH in

comparison to a non-size changing PS colloid reference, reveals striking changes due to the swelling phenomena. Changing pH from 3.70 to 3.00 causes a 20 % increase in PVP colloid radius, and an associated dramatic reduction in translational propulsion velocity to 0 μm s^{-1}, and similar reductions in angular velocity. Over the same pH range PS control particles shows a more modest reduction in velocity, and remain propulsive at pH 3.00. These results were consistent between two different pH modifying acids. The results clearly show that the pH responsive material is able to significantly modulate the propulsion of the Janus colloids within a constant fuel concentration environment. The mechanism for the additional velocity changes is likely to be due to the combined effect of the expected reciprocal relationship between Janus colloidal size and radius, with additional contributions via changes in surface mobility associated with the swelling.

Based on these experimental observations, we performed a comparative simulation of the time dependant statistical accumulation behaviour of the two colloidal types in a 3D spherical pH gradient. The additional velocity modulations due to the size changing response resulted in a considerable prolonged accumulation of PVP colloids in the gradient region, compared to control particles that exhibit no size change, with up to a 6 times increase in accumulated density being observed within the spherical region after 30 minutes. These simulations considerably expand on our previous study, where the effect of pH variations on colloidal motion was inferred from existing theory in the absence of experimental data.[15] In fact our experiments reveal that the modulation in velocity in the realised system is more significant than predicted, due to the associated changes in colloidal surface properties. Additionally, the modulation of Brownian rotational diffusion rate associated with these size changes used as a basis for the previous simulation is verified here, but is convoluted with unavoidable rotational propulsion. Experimental investigation also showed that the PVP colloids could absorb a model cargo dye molecule, and that the rate of dye molecule release doubled over the same pH change that caused the carrier particles to lose their propulsion and become diffusive (pH 3.70 to pH 3.00). A simulation of dye accumulation within a pH gradient showed that the time-scales of pH modulated drug release and particle accumulation are compatible, with a relative enhancement of dye accumulation of 30 times predicted in low pH regions after 2 hours. Taken together, it is clear that investigations of this system supports the tantalising prospect of an active Janus colloid performing targeted smart delivery of stored molecules, using responsive swelling phenomena to provide a mechanism for both spatial accumulation via motion modulation, and simultaneous enhancement of release rate in the desired delivery locations.

The use of lactic acid, during the experimental investigation, a real bio-marker found in the vicinity of tumour cells,[28] signposts that this mechanism could function to locate and deliver cargo at a therapeutic target. However, clearly the reliance on the platinum – hydrogen peroxide system for this demonstration will prevent direct application in this context at present. We envision endeavours in active colloid research to address these fuel incompatibilities within biological systems could be combined with using responsive colloids as described here, to making devices with practical applications for the smart delivery of drugs. Specifically, we highlight advances in the use of enzymatic propulsion systems,[19,29] and note that the concept we demonstrate here could be applied in combination with these propulsive systems. Replacing Pt metal with enzymes may also remove some of the difficulties associated with combining a structurally rigid catalyst into a responsive polymer. In the shorter term, the ability to release cargo molecules from carriers that can accumulate in positions spatially defined by local gradients could be useful for applications in many other solution environments, e.g. to neutralise environmental threats[30]. This function can also be used within lab-on-a chip microfluidic devices. For example it is often desirable to be able to collect a cargo (e.g. a medical diagnostic analyte), move it to a particular location within a device, and then release it for further chemical transformations, such as labelling to allow detection.

Experimentally verifying the collective behaviour simulated here is challenging due to difficulties in producing stable flow free pH gradients, observing high densities of chemically powered colloids due to convective flow,[31] fuel depletion[32] and the gas phase products associated with many driving reactions. However, there is potential to look for similar collective effects in responsive colloidal systems driven by other mechanisms.[33] Finally, the simulation we performed has used a simple model for interactions between nearby colloids, whereas in real high density systems, additional interactions mediated by local self-generated fuel gradients[34] and hydrodynamics are present.[35] Indeed these may allow exquisite structural organisation within accumulations of colloids generated by the pH responsive mechanisms investigated here.

References

[1] J. Howse, R. Jones, A. Ryan, T. Gough, R. Vafabakhsh, R. Golestanian, *Phys. Rev. Letts.* **2007**, *99*, 8.

[2] S. J. Ebbens, Active colloids: Progress and challenges towards realising autonomous applications. *Curr. Opin. Colloid Interface Sci.* **2016**, *21*, 14–23.

[3] J. Wang, *Lab Chip* **2012**, *12*, 1944.

[4] R. Maria-Hormigos, B. Jurado-Sánchez, A. Escarpa, *Lab Chip* **2016**, *16*, 2397.

[5] K. K. Dey, F. Wong, A. Altemose, A. Sen, *Curr. Opin. Colloid Interface Sci.* **2016**, *21*, 4.

[6] S. J. Ebbens, D. A. Gregory, *Acc. Chem. Res.* **2018**, *51*, 1931.

[7] L. Baraban, D. Makarov, R. Streubel, I. Mönch, D. Grimm, S. Sanchez, O. G. Schmidt, *ACS Nano* **2012**, *6*, 3383.

[8] A. I. Campbell, S. J. Ebbens, *Langmuir* **2013**, *29*, 14066.

[9] S. Das, A. Garg, A. I. Campbell, J. R. Howse, A. Sen, D. Velegol, R. Golestanian, S. J. Ebbens, *Nat. Commun.* **2015**, *6*.

[10] J. Simmchen, J. Katuri, W. E. Uspal, M. N. Popescu, M. Tasinkevych, S. Sánchez, *Nat. Commun.* **2016**, *7*, 10598.

[11] H. C. Berg, *Annu. Rev. Biophys. Bioeng.* **1975**, *4*, 119.

[12] L. E. Gerweck, K. Seetharaman, *CANCER Res.* **1996**, *56*, 1194.

[13] Y. Hong, N. Blackman, N. Kopp, A. Sen, D. Velegol, *Phys. Rev. Letts.* **2007**, *99*, 1.

[14] L. Baraban, S. M. Harazim, S. Sanchez, O. G. Schmidt, *Angew. Chemie - Int. Ed.* **2013**, *52*, 5552.

[15] S. J. Ebbens, G. A. Buxton, A. Alexeev, A. Sadeghi, J. R. Howse, *Soft Matter* **2012**, *8*, 3077.

[16] J. Burdick, R. Laocharoensuk, P. M. Wheat, J. D. Posner, J. Wang, *J. Am. Chem. Soc.* **2008**, *130*, 8164.

[17] S. Balasubramanian, D. Kagan, C.-M. J. Hu, S. Campuzano, M. J. Lobo-Castañon, N. Lim, D. Y. Kang, M. Zimmerman, L. Zhang, J. Wang, *Angew. Chem. Int. Ed. Engl.* **2011**, *50*, 4161.

[18] X. Ma, K. Hahn, S. Sanchez, *J. Am. Chem. Soc.* **2015**, 150410110204000.

[19] X. Ma, S. Sánchez, *Tetrahedron* **2017**, *73*, 4883.

[20] R. Golestanian, T. B. Liverpool, A. Ajdari, *New J. Phys.* **2007**, *9*, 126.

[21] Y. Kato, S. Ozawa, C. Miyamoto, Y. Maehata, A. Suzuki, T. Maeda, Y. Baba, *Cancer Cell Int.*

2013, *13*, 1.

[22] D. Dupin, S. Fujii, S. P. Armes, P. Reeve, S. M. Baxter, *Langmuir* **2006**, *22*, 3381.

[23] S. Ebbens, R. A. L. Jones, A. J. Ryan, R. Golestanian, J. R. Howse, *Phys. Rev. E - Stat. Nonlinear, Soft Matter Phys.* **2010**, *82*.

[24] G. Dunderdale, S. Ebbens, P. Fairclough, J. Howse, *Langmuir* **2012**, *28*.

[25] A. J. Morse, S. P. Armes, P. Mills, R. Swart, **2013**, *29*, 15209.

[26] R. J. Archer, A. J. Parnell, A. I. Campbell, J. R. Howse, S. J. Ebbens, *Adv. Sci.* **2017**, *1700528*, 1700528.

[27] S. Ebbens, M.-H. Tu, J. R. Howse, R. Golestanian, *Phys. Rev. E. Stat. Nonlin. Soft Matter Phys.* **2012**, *85*, 020401.

[28] M. Stubbs, P. M. McSheehy, J. R. Griffiths, *Adv. Enz. Reg.* **1999**, *39*, 13.

[29] X. Ma, X. Wang, K. Hahn, S. Sánchez, *ACS Nano* **2016**, *10*, 3597.

[30] J. Parmar, D. Vilela, K. Villa, J. Wang, S. Sánchez, *J. Am. Chem. Soc.* **2018**, *140*, 9317.

[31] D. A. Gregory, S. J. Ebbens, *Langmuir* **2018**, *34*, 4307.

[32] A. Brown, W. Poon, *Soft Matter* **2014**, 4016.

[33] R. Dong, Q. Zhang, W. Gao, A. Pei, B. Ren, *ACS Nano* **2015**, acsnano.5b05940.

[34] S. Saha, R. Golestanian, S. Ramaswamy, *Phys. Rev. E - Stat. Nonlinear, Soft Matter Phys.* **2014**, *89*, 1.

[35] A. I. Campbell, S. J. Ebbens, P. Illien, R. Golestanian, *Nat. Commun.* **2019**, *10*, 1.